Quantitative Phosphoproteomics Dissection of Seven-transmembrane Receptor Signaling Using Full and Biased Agonists*[S]

Gitte L. Christensen‡§¶‖, Christian D. Kelstrup‖**‡‡, Christina Lyngsø‡§, Uzma Sarwar¶, Rikke Bøgebo¶, Søren P. Sheikh§§, Steen Gammeltoft¶, Jesper V. Olsen**‡‡¶¶, and Jakob L. Hansen‡§‖‖

Seven-transmembrane receptors (7TMRs) signal through the well described heterotrimeric G proteins but can also activate G protein-independent signaling pathways of which the impact and complexity are less understood. The angiotensin II type 1 receptor (AT_1R) is a prototypical 7TMR and an important drug target in cardiovascular diseases. "Biased agonists" with intrinsic "functional selectivity" that simultaneously blocks $G\alpha_q$ protein activity and activates G protein-independent pathways of the AT_1R confer important perspectives in treatment of cardiovascular diseases. In this study, we performed a global quantitative phosphoproteomics analysis of the AT_1R signaling network. We analyzed ligand-stimulated SILAC (stable isotope labeling by amino acids in cell culture) cells by high resolution (LTQ-Orbitrap) MS and compared the phosphoproteomes of the AT_1R agonist angiotensin II and the biased agonist [Sar^1,Ile^4,Ile^8]angiotensin II (SII angiotensin II), which only activates the $G\alpha_q$ protein-independent signaling. We quantified more than 10,000 phosphorylation sites of which 1183 were regulated by angiotensin II or its analogue SII angiotensin II. 36% of the AT_1R-regulated phosphorylations were regulated by SII angiotensin II. Analysis of phosphorylation site patterns showed a striking distinction between protein kinases activated by $G\alpha_q$ protein-dependent and -independent mechanisms, and we now place protein kinase D as a key protein involved in both $G\alpha_q$-dependent and -independent AT_1R signaling. This study provides substantial novel insight into angiotensin II signal transduction and is the first study dissecting the differences between a full agonist and a biased agonist from a 7TMR on a systems-wide scale. Importantly, it reveals a previously unappreciated diversity and quantity of $G\alpha_q$ protein-independent signaling and uncovers novel signaling pathways. We foresee that the amount and diversity of G protein-independent signaling may be more pronounced than previously recognized for other 7TMRs as well. Quantitative mass spectrometry is a promising tool for evaluation of the signaling properties of biased agonists to other receptors in the future. *Molecular & Cellular Proteomics 9:1540–1553, 2010.*

Seven-transmembrane receptors (7TMRs)[1] constitute the largest family of plasma membrane receptors. These receptors regulate a variety of biological processes and are currently the most prominent therapeutic targets, highlighted by an abundance of clinically available drugs (1–5). Their cellular responses were until recently thought to depend primarily on G protein activation and generation of second messengers such as inositol 1,4,5-trisphosphate, diacylglycerol, and cAMP, reflected by the term G protein-coupled receptors. However, the 7TMR structure also confers activation of G protein-independent signaling initiated by direct interaction with β-arrestin or tyrosine kinases (1–3, 6, 7). The discovery of alternative signaling pathways to the G protein-initiated pathways has also led to the discovery of regulatory peptides that can have agonistic effects on one pathway while simultaneously antagonizing another. Such pharmacological separation of signaling pathways has an enormous clinical potential,

From the ‡Laboratory for Molecular Cardiology, Danish National Research Foundation Centre for Cardiac Arrhythmia, Department of Biomedical Sciences and ‡‡Novo Nordisk Foundation Center for Protein Research, Faculty of Health Sciences, University of Copenhagen, Blegdamsvej 3b, DK-2200 Copenhagen, Denmark, §Copenhagen University Hospital, Rigshospitalet, Juliane Mariesvej 20, section 9302, DK-2100 Copenhagen, Denmark, ¶Department of Clinical Biochemistry, Glostrup Hospital, Nordre Ringvej, DK-2600 Glostrup, Denmark, **Department of Proteomics and Signal Transduction, Max Planck Institute for Biochemistry, Am Klopferspitz 18, D-82152 Martinsried, Germany, and §§Department for Biochemistry, Pharmacology and Genetics, Odense University Hospital, University of Southern Denmark, Soendre Boulevard 29, DK-5000 Odense, Denmark

Received, November 13, 2009, and in revised form, March 31, 2010
Published, MCP Papers in Press, April 2, 2010, DOI 10.1074/mcp.M900550-MCP200

[1] The abbreviations used are: 7TMR, seven-transmembrane receptor; Ang II, angiotensin II; AT_1R, angiotensin II type 1 receptor; SII Ang II, [Sar^1,Ile^4,Ile^8]Ang II where Sar is sarcosine; SILAC, stable isotope labeling by amino acids in cell culture; LTQ-Orbitrap, linear ion trap orbitrap mass spectrometer; PKC, protein kinase C; PKD, protein kinase D; HEK293, human embryonic kidney cell line; AT_1R-HEK, AT_1R stable transfected HEK293; GEF, guanine nucleotide exchange factor; Erk, extracellular signal-regulated kinase; DMEM, Dulbecco's modified Eagle's medium; SCX, strong cation exchange; FPLC, fast protein LC; MSA, multistage activation; FDR, false discovery rate; EGF, epidermal growth factor; FGF, fibroblast growth factor; PDCD4, programmed cell death protein 4; ROCK, Rho-associated protein kinase.

which is described by pharmacological concepts such as "functional selectivity" or "biased agonism" (3, 8, 9). A number of antagonists have only been evaluated by G protein-dependent readouts and may therefore turn out to be biased agonists. An example of such biased agonism is the retrospective discovery that the widely used inverse β_2-adrenergic receptor agonist carvedilol, which has been superior to other β-blockers in the prevention of heart failure, functions as a biased agonist. The reason for the increased survival of patients treated with carvedilol is unclear, but this drug acts as a biased agonist by activating the Erk1/2 mitogen-activated protein kinases while inhibiting $G\alpha_s$-mediated effects (10). This could be the explanation behind its clinical success because the G protein-independent signaling could confer the effects that improve survival (10). Similar mechanisms are likely to underlie the molecular mechanism behind other successful 7TMR drugs. Comparable observations that G protein-independent signaling may provide beneficial effects have been made in model systems for angiotensin II (Ang II) signaling via the Ang II type 1 receptor (AT_1R). The AT_1R is commonly used as a model system to study $G\alpha_q$-dependent *versus* -independent signaling because of the availability of excellent and well defined biological tools for this receptor.

The AT_1R serves as a key regulator of cardiovascular physiology, maintaining salt and fluid homeostasis and blood pressure (11, 12). The AT_1R is also involved in a number of medical conditions including endothelial dysfunction and atheroma, cardiac hypertrophy and failure, atrial fibrillation, nephropathy, insulin resistance, and cancer (13) and is therefore a prominent drug target in cardiovascular diseases, reflected by the common use of AT_1R blockers such as losartan and angiotensin-converting enzyme inhibitors, for example ramipril. AT_1R signaling is particularly interesting with respect to functional selectivity because selective activation of $G\alpha_q$ protein-independent signaling has proven relevant in primary cells, in isolated organs, and *in vivo* (3, 14, 15).

AT_1R signaling pathways encompass a complex network of signaling molecules including heterotrimeric G proteins, protein kinases, and scaffold proteins (11, 12). The biased agonist [Sar^1,Ile^4,Ile^8]Ang II (SII Ang II) is a well established AT_1R ligand that provides the opportunity to study $G\alpha_q$-independent effects (16). SII Ang II selectively inhibits the $G\alpha_q$ protein signaling branch while still activating the remaining network that is activated from the AT_1R such as tyrosine kinase signaling (6, 7), β-arrestin signaling (16), and the possibly minor contribution from other trimeric G proteins such as $G_{12/13}$, G_i, and G_o (17–19) that collectively is called $G\alpha_q$-independent signaling (Fig. 1*A*). Activation of Erk1/2 has been thoroughly investigated with respect to $G\alpha_q$ protein-dependent *versus* β-arrestin-dependent signaling (20–22). These studies have established that Erk1/2 is activated by both pathways and furthermore that there is a striking pathway-dependent difference in the function and localization of activated Erk1/2 (20). $G\alpha_q$-dependent activation of Erk1/2 results in nuclear translocation and gene transcription, whereas $G\alpha_q$-independent activation leads to a tight association with β-arrestin, which results in cytosolic sequestration of Erk1/2 (20–22). This difference in Erk1/2 localization has been related to several important phenotypic differences. The β-arrestin part of $G\alpha_q$-independent signaling has been linked to cellular survival and renewal as well as regulation of cell migration (23, 24). Conversely, the $G\alpha_q$ protein-mediated component of AT_1R signaling has been associated with cellular death and fibrosis leading to cardiac hypertrophy and progression to heart failure (3). These divergent roles of the two signaling pathways indicate that full therapeutic blockade of the AT_1R may have drawbacks in some situations due to blocking desirable physiological functions. Biased agonism provides a novel pharmacological potential as the use of biased agonists may allow selective blocking of undesired effects while maintaining desired effects (2, 3).

Global and site-specific analysis of *in vivo* phosphorylation sites by quantitative mass spectrometry has emerged as the method of choice to investigate cell signaling pathways in an unbiased fashion (25). In this study, we characterized the AT_1R signaling network by high resolution quantitative phosphoproteomics and thereby delineated the differences between the full agonist Ang II and the biased agonist SII Ang II. To characterize the AT_1R signaling network, we used stable isotope labeling by amino acids in cell culture (SILAC) in combination with phosphopeptide enrichment and high performance mass spectrometry (26). This approach has become increasingly powerful in the analysis of signaling pathways because it allows for a high throughput and quantitative mapping of changes in cellular protein phosphorylation on a systems-wide scale. The majority of the identified proteins in our study have not previously been associated with AT_1R signaling, and we found $G\alpha_q$ protein-independent signaling to play an unexpected large role in AT_1R signaling.

EXPERIMENTAL PROCEDURES

Cell Culture, Inositol Accumulation, and Western Blotting

AT_1R stable transfected HEK293 (AT_1R-HEK) cells were a generous gift from Robert J. Lefkowitz, Duke University Medical Center, Durham, NC (24). Cells were maintained in DMEM (Lonza) supplemented with 10% FCS (Invitrogen), 50 units/ml penicillin, 50 units/ml streptomycin (Lonza), 2 mM glutamine (Sigma), and 300 μg/ml Zeocin (Invitrogen). AT_1R-HEK cells were starved overnight in serum-free DMEM and stimulated with 100 nM Ang II (Sigma) or 18.7 μM SII Ang II (Cleveland Clinic). Gö6983, rottlerin, and Y27632 were added to the cells 30 min before onset of an experiment. Equal amounts of lysates were loaded on SDS gels (Pagegel Inc.), and Western blotting was performed as wet blotting. Briefly, PVDF membranes (Amersham Biosciences) were soaked in ethanol and placed in cold transfer buffer (25 mM Tris-HCl, 195 mM glycine, 20% ethanol, 0.1% SDS). Proteins were transferred in a Criterion blotter (Bio-Rad). Membranes were blocked using Enhanced ECL blocking reagent and probed against phosphorylated Erk1/2 and total Erk1/2 or phosphorylated PKD Ser^{910} (Cell Signaling Technology, Inc.). Protein bands were visualized using enhanced ECL (Amersham Biosciences) and scanned in an Intelligent Dark Box II (Fuji). Inositol production was

measured in the presence of *myo*-[2-^{3}H]inositol (Amersham Biosciences). Briefly, AT_1R-HEK cells were seeded into 48-well plates coated with 0.25% poly-L-lysine (100,000 cells/well) and incubated in inositol-free DMEM (Invitrogen) supplemented with *myo*-[2-^{3}H]-inositol (1 μCi/ml). Twenty hours after application of the radioligand, the cells were assayed as described previously (28). For SILAC labeling, three populations of AT_1R-HEK cells were SILAC-encoded with L-arginine and L-lysine, L-[U-$^{13}C_6$]arginine and L-[$^2H_4$]lysine, or L-[U-$^{13}C_6$,$^{15}N_4$]arginine and L-[U-$^{13}C_6$,$^{15}N_2$]lysine and treated with vehicle, 100 nM Ang II, or 18.7 μM SII Ang II, respectively (amino acids were from Cambridge Isotope Laboratories; SILAC medium was from HyClone). Cells were lysed in a modified radioimmune precipitation assay buffer (1% Nonidet P-40, 0.1% sodium deoxycholate, 150 mM NaCl, 1 mM EDTA, 50 mM Tris, pH 7.5, 10 mM β-glycerol phosphate, 10 mM NaF, one Complete® inhibitor mixture tablet/50 ml) and mixed 1:1:1 based on total protein concentration. Proteins were precipitated in 4× excess of ice-cold acetone. We performed a complete biological replicate of all SILAC experiments.

PKD Kinase Assays

AT_1R-HEK cells were stimulated as described above and lysed on ice for 15min in lysis buffer (0.5% Triton X-100, 150 mM NaCl, 50 mM Tris-HCl, pH 7.4, 1 mM Na_3VO_4, 5 mM EDTA, 50 mM NaF, 10 nM calyculin A, 10 μM leupeptin, 5 μM pepstatin, 1 μg/ml aprotinin). Lysates were cleared for 15 min at 13,000 rpm. Immunoprecipitation was performed by addition of 1.5 μg of PKD antibody (Santa Cruz Biotechnology, Inc.) for 1 h followed by 1-h addition of Protein G-agarose beads. The beads were washed three times with lysis buffer and twice in kinase buffer (45 mM Tris-HCl, pH 7.4, 15 mM $MgCl_2$, 1.5 mM dithiothreitol) and resuspended in 20 μl of kinase buffer. The kinase reaction was initiated by addition of 10 μl of reaction buffer (450 μM ATP, 0.25 μg/μl syntide 2 (PLARTLSVAGLPGKK), 0.2 μCi of [γ-^{32}P]ATP), and phosphorylation was allowed under vigorous shaking for 10 min at 30 °C. 20 μl of the kinase reaction were spotted onto phosphocellulose paper (Whatman p81), and the paper was washed with 150 mM orthophosphoric acid. Phosphorylation of syntide 2 was determined by autoradiography on a STORM™ phosphorimaging system using ImageQuant™ software (GE Healthcare).

Sample Preparation for Mass Spectrometry

In-solution Digestion

The acetone-precipitated lysate was resolubilized in an 8 M urea buffer (6 M urea + 2 M thiourea in 10 mM HEPES, pH 8). The soluble proteins were reduced for 30 min at room temperature with 1 mM DTT and alkylated for 15 min by 5.5 mM iodoacetamide. Endoproteinase Lys-C (Wako) was added at 1:100 (w/w), and the lysates were digested for 4 h at room temperature. The resulting peptide mixtures were diluted 4-fold with deionized water to achieve a final urea concentration below 2 M. Trypsin (modified sequencing grade, Promega) was added at 1:100 (w/w), and the sample was digested overnight. Trypsin and Lys-C activity was quenched by acidification of the reaction mixtures with a 10% TFA solution to pH ~2. The peptide mixture was desalted and concentrated on a C_{18} SepPak cartridge (Waters) and eluted with 2 × 1 ml of 60% ACN in 0.3% TFA.

Proteins from the insoluble chromatin pellet were extracted by repeated incubations in a mixture of 8 M urea and Benzonase (Merck). The extracted proteins were treated, digested, and purified by the same approach as the acetone precipitate above.

Strong Cation Exchange Chromatography

Peptide fractionation by strong cation exchange (SCX) chromatography was performed to reduce the complexity of the peptide mixture. The in-solution digests were loaded onto an SCX column (1-ml Resource S, GE Healthcare) using an Äkta FPLC system (GE Healthcare). Peptides were separated by a linear gradient for 30 min from 100% buffer A (5 mM KH_2PO_4, pH 2.7, 30% ACN) to 30% buffer B (350 mM KCl, 5 mM KH_2PO_4, pH 2.7, 30% ACN) with a flow rate of 1 ml/min. Fractions were collected every minute using a fraction collector. In total, 16 SCX fractions including the column flow-through were collected for further analysis.

Phosphopeptide Enrichment

Phosphopeptides were enriched using Titansphere chromatography as described (26). Briefly, phosphopeptides were enriched on titanium dioxide beads (10-μm Titansphere, GL Sciences) precoated with 2,5-dihydroxybenzoic acid. 5 μg of coated-beads were added to each SCX fraction and incubated with rotation for 15 min. The beads were washed once with 200 μl of 30% ACN in 3% TFA and once with 200 μl of 60% ACN in 0.3% TFA and transferred in 200 μl of 75% acetonitrile in 0.3% TFA on top of a reversed phase C_8 StageTip. The bound phosphopeptides were eluted directly into a 96-well plate by 2 volumes of 20 μl of 25% ACN in 15% NH_4OH, water (pH > 11). The eluates were immediately dried in a SpeedVac at 60 °C.

Mass Spectrometric Analysis

LC-MS/MS

The dried phosphopeptide mixtures were acidified with 5% acetonitrile in 0.3% TFA to an end volume of 8 μl and analyzed by on-line nanoflow LC-MS/MS as described previously (26) with a few modifications. Briefly, all nano-LC-MS/MS experiments were performed on an EASY-nLC™ system (Proxeon Biosystems, Odense, Denmark) connected to the LTQ-Orbitrap XL (Thermo Electron, Bremen, Germany) through a nanoelectrospray ion source.

The tryptic peptide and phosphopeptide mixtures were separated in a 15-cm analytical column (75-μm inner diameter) in house-packed with 3-μm C_{18} beads (Reprosil-AQ Pur, Dr. Maisch) with a 90-min gradient from 5 to 30% acetonitrile in 0.5% acetic acid. The effluent from the HPLC was directly electrosprayed into the mass spectrometer.

The MS instrument was operated in data-dependent mode to automatically switch between full-scan MS and MS/MS acquisition. Survey full-scan MS spectra (from *m/z* 300 to 2000) were acquired in the orbitrap with resolution $R = 60{,}000$ at *m/z* 400 (after accumulation to a "target value" of 1e6 in the linear ion trap). The 10 most intense peptide ions with charge states ≥2 were sequentially isolated to a target value of 5e3 and fragmented in the linear ion trap by multistage activation (MSA; or pseudo-MS3) (26, 29) All fragment ion spectra were recorded with the LTQ detectors. For all measurements with the orbitrap detector, a lock mass ion from ambient air (*m/z* 445.120024) was used as an internal calibrant as described (30). Typical mass spectrometric conditions were as follows: spray voltage, 2.4 kV; no sheath and auxiliary gas flow; heated capillary temperature, 150 °C; normalized collision energy, 35% for MSA in the LTQ with wideband activation enabled. The ion selection threshold was 500 counts for MS2, and the maximum allowed ion time was 500 ms for full scans and 150 ms for MS/MS. An activation *q* of 0.25 and activation time of 30 ms were used. For MSA, neutral losses of *m/z* 32.66, 48.99, and 97.97 were activated.

Raw MS Data Analysis

Peptide Identification by Mascot and MaxQuant—Raw Orbitrap full-scan MS and ion trap MSA spectra were processed by MaxQuant as described (31). In brief, all identified SILAC triplets were quantified, accurate precursor masses were determined using the entire LC

elution profiles, and MS/MS spectra were filtered to contain at most six peaks per 100-Da interval and merged into peak list files (*.msm).

Peptides and proteins were identified by Mascot (Matrix Science, London, UK) via automated database matching of all tandem mass spectra against an in-house curated concatenated target/decoy database, a forward and reversed version of the human International Protein Index sequence database (version 3.37, 138,632 forward and reversed protein sequences from the European Bioinformatics Institute) supplemented with common contaminants such as human keratins, bovine serum proteins, and porcine trypsin. Tandem mass spectra were initially matched with a mass tolerance of 7 ppm on precursor masses and 0.5 Da for fragment ions and strict trypsin specificity, allowing for up to three missed tryptic cleavage sites. *N*-Pyroglutamine (Gln +17.026549 Da), oxidized methionine (+15.994915 Da), acetylation of protein (N terminus +42.010565 Da), and phosphorylation of serine, threonine, and tyrosine (Ser/Thr/Tyr +79.966331 Da) were searched as variable modifications.

Peptide Filtering, Quantitation, and Phosphosite Localization by MaxQuant—The resulting Mascot result files (*.dat) were loaded into the MaxQuant software suite version 1.0.12.35 for further processing. By automatically filtering on peptide length, mass error precision estimates, and Mascot score of all forward and reversed peptide identifications, we fixed the estimated false discovery rate (FDR) of all peptide and protein identifications at 1% using a Bayesian approach as detailed previously (32). The FDR is a framework to address the multiple hypothesis testing problem by restricting the number of false positives to a fixed percentage as opposed to *e.g.* a fixed Mascot score threshold. The database setup and FDR estimation are equivalent to those in Ref. 33; additional variable modifications in the search algorithm were used to increase the search space. Ratio determination by MaxQuant was done by robust linear regression of the two-dimensional centroid values of the intensity/time elution profiles for all isotope distributions that were present in the different SILAC states to determine the overall ratio difference. To pinpoint the actual phosphorylated amino acid residue(s) within all identified phosphopeptide sequences in an unbiased manner, MaxQuant calculated the localization probabilities of all putative serine, threonine, and tyrosine phosphorylation sites using the post-translation modification score algorithm as described (26). For final ratio calculation, MaxQuant calculates the median of all peptide ratios associated with a specific phosphorylation site including variants such as oxidation of methionine and missed cleavages. As a last filter, only sites with a localization probability >75% and a post-translation modification delta score of at least 5 were included in the analysis. The extensively annotated spectra showing multiple water and phosphopeptide losses (34) explain more than 70% of the fragment ions (supplemental Fig. X). All spectra can be found in supplemental Data IX.

The determined regulation of a specific phosphorylation site identified in this study is most likely not related to the Mascot score as ratio information is not included in the identification step. To verify this, we plotted the Mascot score distributions and localization probability distributions from the phosphopeptides we report as regulated and compared them with those not reported as regulated (supplemental Fig. XI). As illustrated, the distributions overlapped almost completely, indicating that there indeed is no relation between identification and showing a significant ratio.

Cutoffs, Phosphorylation Site Annotation, and Analysis—The two biological replicates and the two time points were considered as four independent experiments. Phosphopeptides were required to have at least two independent ratios above the cutoff to be considered reproducibly regulated. This method ensures that peptides identified across all four conditions are also more accurately measured in the individual experiments because of a higher peptide count. The cutoff was set at 3 times the median standard deviation of the log-transformed ratios of the phosphorylated peptides. The ratios of the non-phosphorylated peptides were used to estimate the proportion of false positives as shown in Fig. 2*B*. The final cutoff was set at a ratio of 1.5 observed in at least two experiments, which provides an estimated 0.3% false positive rate.

Regulated phosphosites were annotated with UniProt accession numbers and compared with UniProt, PHOSIDA, and Phospho.ELM databases of known phosphosites (supplemental Tables I and II). We evaluated whether a phosphorylated protein was previously observed to be regulated by Ang II by searching for reports in PubMed (supplemental Tables I and II). Functional grouping of regulated proteins was done manually. All regulated sites are shown in supplemental Table IV, and all the detected phosphosites are shown in supplemental Table V. All identified proteins are listed in supplemental Table VII, and all modified peptides are listed in supplemental Table VIII.

Phosphosite Sequence Motif Logo Plots—To identify enriched sequence motifs in the phosphorylation site data set, we made use of an in-house algorithm that iteratively tests for position-specific over-representation of any amino acid groups in a prealigned list of the regulated sequences compared with the average occurrence of the amino acid group in a list of sequences surrounding non-regulated phosphosites. In each round of iteration, the most significant amino acid group is excluded in a position-specific fashion from both lists (35). Statistically significant over-representation is calculated using the R (a programming language and software environment for statistical computing and graphics) implementation of Fisher's exact test. Grouping of amino acids was done on the basis of related chemical properties (acidic, basic, aromatic, aliphatic, hydrophilic, amide, polar, and cyclic). The Perl package of WebLogo was used internally in the algorithm to visualize the enriched sequence motifs as logo plots. For the kinase motif analysis, we used a sequence window of ±6 amino acids surrounding the central phosphorylated serine, threonine, or tyrosine residue. All up-regulated phosphorylation site sequences were compared with non-regulated phosphorylation site sequences from the results from either Ang II or SII Ang II, respectively. We considered a motif significant if it fulfilled our conservative cutoff of $p < 0.001$ on the Bonferroni correction-adjusted p values.

RESULTS

Dissecting AT_1R Signaling by Mass Spectrometry—To identify novel proteins in the AT_1R signaling network and determine the weight and nature of $G\alpha_q$-dependent and -independent signaling, we used SILAC combined with phosphopeptide enrichment and high resolution mass spectrometry. This approach simultaneously enables high throughput and quantitative analysis of changes in multiple protein phosphorylation sites (26). We compared AT_1R-HEK cells incubated with and without Ang II and SII Ang II. Ang II stimulation fully activates the AT_1R, whereas SII Ang II stimulation only activates the β-arrestin-dependent and other $G\alpha_q$ protein-independent signaling events (16, 20). As can be seen from Fig. 1*B*, SII Ang II was unable to induce inositol accumulation (a readout for $G\alpha_q$ activity) but could still activate Erk1/2, which has previously been shown to be β-arrestin-dependent (20) (Fig. 1*B*).

Two pools of triple SILAC-labeled cells were stimulated with vehicle, Ang II, and SII Ang II for 3 or 15 min, and these experiments were repeated as biological, independent repli-

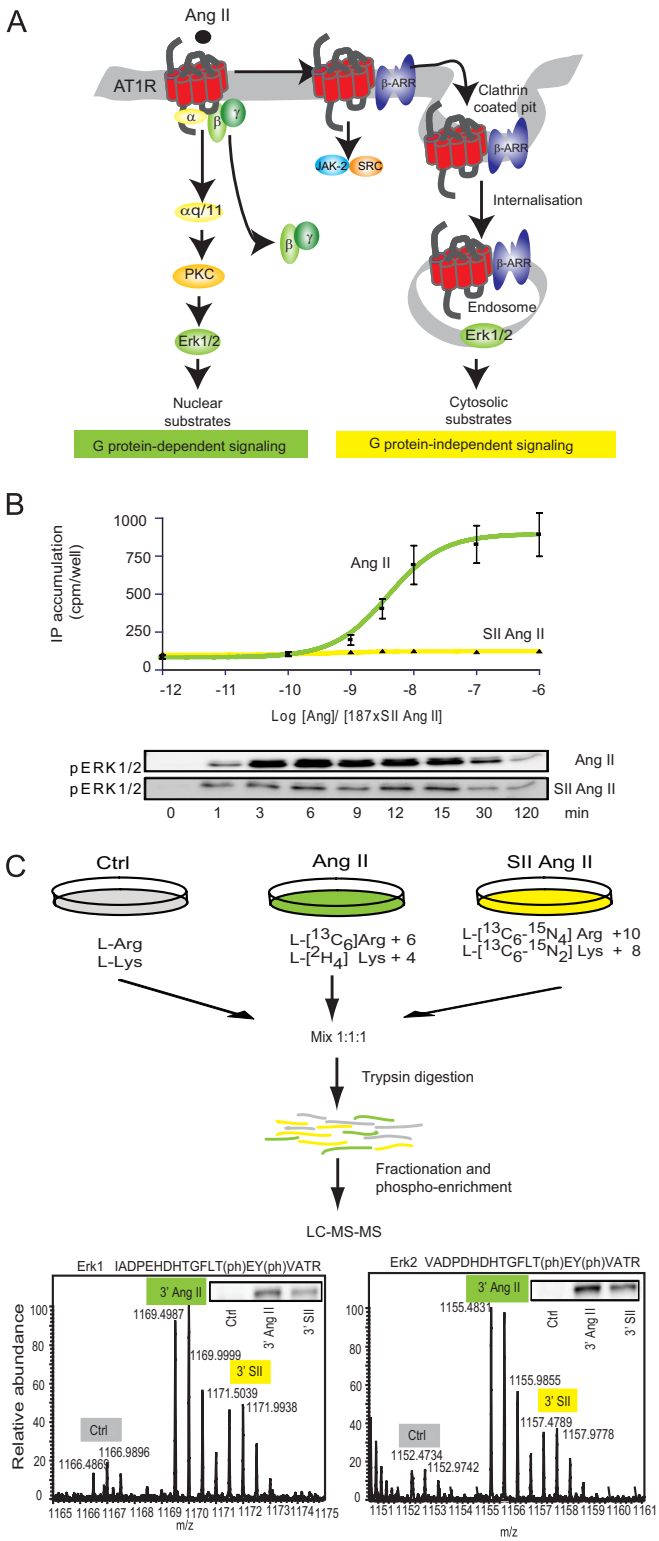

FIG. 1. **Experimental setup.** *A*, illustration showing the principle signaling pathways from the AT_1R. The AT_1R associates with heterotrimeric G proteins but can also signal through G protein-independent mechanisms, which include direct binding to tyrosine kinases or signaling complexes scaffolded by β-arrestin (*β-ARR*). Regulation of Erk1/2 is well described in this system and characterized by differential localization upon G protein-dependent and -independent activation. *B*, SII Ang II mediates $G\alpha_q$-independent Erk1/2 activation in AT1R-HEK cells. *Upper panel*, dose-response curves for agonist-induced inositol phosphate (*IP*) accumulations are shown as a mean of three independent experiments performed in triplicate. Data are depicted in cpm/well (±S.E.). The concentration of SII Ang II was 187 times the concentration of Ang II due to equally lower binding affinity (16). *Lower panel*, Western blot analysis of Ang II- and SII Ang II-induced Erk1/2 activation as a function of time. Data are presented as the mean and error bars reflect ± S.E. of four experiments. *C*, the workflow of the quantitative phosphoproteomics approach by SILAC. Three populations of AT_1R-HEK cells were labeled with normal and stable isotope-substituted arginine and lysine, creating proteins and peptides distinguishable by mass. The medium and heavy labeled cell pools were stimulated with 100 nM Ang II or 18.7 μM SII Ang II, respectively (for 3 and 15 min), the cells were lysed, and lysates were mixed 1:1:1. Proteins were digested by trypsin and endoproteinase Lys-C and fractionated by SCX, and phosphopeptides were enriched on TiO_2 columns. The resulting high resolution orbitrap full-scan MS spectra reveal SILAC triplets of each peptide, allowing quantification of hormone-induced changes in the phosphorylation level between the three groups. The 3- and 15-min samples were treated as individual experiments. A phospho-Erk (*pERK*) spectrum is shown to illustrate the high resolution MS spectrum. For comparison, a Western blot of phospho-Erk1/2 on the same lysate is illustrated in the *top right corner*. *Ctrl*, control; *(ph)*, phosphorylation.

cates. Lysates from vehicle-, Ang II-, and SII Ang II-treated cells were mixed, the proteins were enzymatically digested with trypsin and separated into 16 fractions, and phosphopeptides were enriched on TiO_2 columns (26) (Fig. 1*B*). Each fraction was independently analyzed (the last four fractions were combined) by on-line reversed phase nanoflow LC-MS on a hybrid linear ion trap orbitrap mass spectrometer (LTQ-Orbitrap), and phosphopeptides were fragmented by multistage activation ("pseudo-MS3") (26). All SILAC-encoded peptides eluted as characteristic triplets, and their intensities, reflecting the relative phosphorylation state of the peptide, were measured by high resolution orbitrap mass spectrometry (Fig. 1*B*). To validate the reliability of the method, the relative phosphorylation intensities from mass spectrometry analysis were compared with standard Western blotting analysis for selected proteins. As exemplified with Erk1/2, the changes of the peak intensities were comparable with what was observed using phosphosite-specific antibodies (Fig. 1*C*).

AT_1 Receptor Signaling Affects Multiple Cellular Processes: 36% Is Regulated by $G\alpha_q$-independent Signaling—With this approach, we identified 10,965 unique phosphosites with more than 99% certainty of correct peptide identification and 75% certainty of phosphosite localization. These peptides were found on 2661 different proteins, and the distribution of Tyr(P), Thr(P), and Ser(P) was 1.2, 12.0, and 86.8%, respectively, which is comparable with previous observations (26) (Fig. 2, *A* and *C*, and supplemental Table III). The distribution of all up-regulated Tyr(P), Thr(P), and Ser(P) sites was 0.6, 11.1, and 88.3%, respectively (Fig. 2*C* and supplemental Tables I and II),

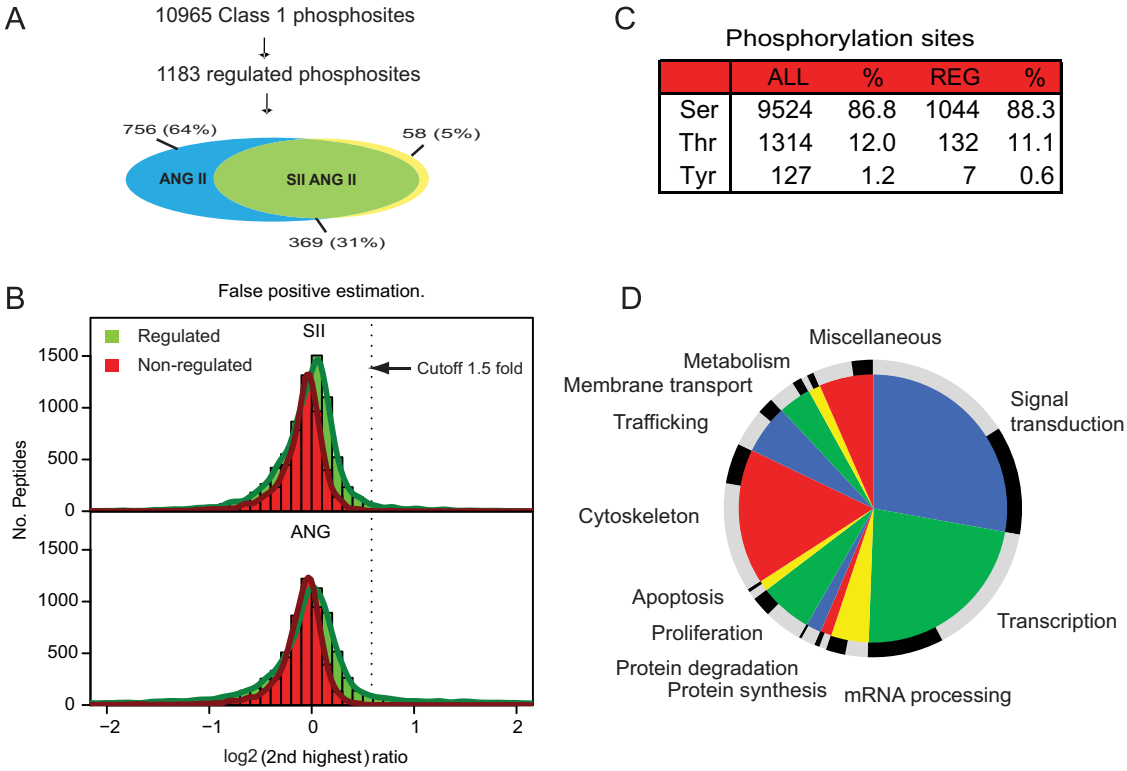

	ALL	%	REG	%
Ser	9524	86.8	1044	88.3
Thr	1314	12.0	132	11.1
Tyr	127	1.2	7	0.6

FIG. 2. **Distribution of phosphopeptides.** *A*, we identified 10,965 unique phosphosites. 1183 of these peptides were reproducibly regulated 1.5-fold by Ang II or SII Ang II after 3- and/or 15-min stimulation. 36% of the AT$_1$R-regulated phosphorylation sites were regulated by SII Ang II. *B*, the cutoff was determined as three standard deviations from the mean, equal to 1.5-fold. Comparing the distribution of non-phosphorylated peptides with that of phosphorylated peptides allowed us to determine a false positive identification rate of 0.3%. *C*, the distribution of all identified serine, threonine, and tyrosine phosphorylation sites compared with the distribution of regulated sites (*REG*). *D*, the 1183 phosphorylation sites were manually grouped in functional groups according to the main known cellular function of the protein on which they reside. The *outer circle* indicates the fraction of phosphorylation sites regulated by Ang II only (*gray*) and by SII Ang II (*black*).

and a similar distribution was seen for the Ang II- and SII Ang II-regulated peptides. The number of phosphorylation sites identified is relatively high compared with other proteomics studies, and therefore the analysis uncovered many novel phosphorylation sites (36–38).

In the following bioinformatics study of our data set, we only analyzed the phosphorylation sites that were up-regulated as our experience is that down-regulation is less reproducible and can be due to both activation of phosphatases and general degradation of protein, which can change the absolute protein concentration much faster than synthesis. The cutoff was set at 3 times the median standard deviation of the log-transformed ratios of the phosphorylated peptides, equal to 1.5-fold. The ratios of all non-phosphorylated peptides detected in the study, which were expected to be unaffected by the short term treatment (ratio of 1:1:1), were used to estimate the proportion of false positives (0.3%) in our regulated set of phosphopeptides as shown on Fig. 2*B*.

1183 phosphosites were found to be regulated; 36% of these or 427 phosphosites were regulated by SII Ang II. This group represents phosphosites that are affected by Gα_q-independent signaling. A smaller group of 58 sites was found to be regulated by SII Ang II but not Ang II; many of these sites are probably also regulated by Ang II but did not reach the threshold.

In general, we found SII Ang II to be a weaker inducer of common phosphorylation sites than Ang II alone. This is not surprising as we and others have previously shown that SII Ang II is only a partial agonist on β-arrestin-dependent signaling as reflected by a weaker recruitment of β-arrestin (8, 39). In this study, SII Ang II was also a weaker inducer than Ang II of almost all phosphorylations (generally 20–50% of the Ang II response). Despite this, we used a 1.5-fold ratio increase as the cutoff for both Ang II and SII Ang II. However, the impact of AT$_1$R-mediated Gα_q-independent signaling may be underestimated because phosphosites that are only regulated 1.5–3-fold with Ang II might also be regulated by SII Ang II but fall under the cutoff. Using these parameters, we found 1183 up-regulated phosphorylation sites on 527 phosphoproteins. For some phosphosites, SII Ang II stimulation yielded 50% of Ang II stimulation and on some sites only 20%. This difference could indicate that some of the Ang II-regulated phosphosites are affected by both Gα_q-dependent and -independent signaling, whereas others are strictly Gα_q-independent. An example of this is the well described Erk1/2 kinases discussed above in which activation loop phosphorylation sites were regulated about 20-

fold with Ang II but only 4-fold with SII Ang II. Erk1/2 are in fact regulated by both $G\alpha_q$-dependent and -independent pathways. Thus, SII Ang II only affects the $G\alpha_q$-independent pathway and moreover is a partial agonist on this pathway, and thus SII Ang II only yielded 20% of the regulation observed with Ang II. For other kinases such as CAMK2D, SII Ang II up-regulated phosphorylation sites to around 50% of Ang II induction, indicating that $G\alpha_q$-independent signaling is dominant for regulation of this protein.

The present study adds substantially to uncovering the Ang II signaling network as more than 80% of these phosphoproteins have not previously been linked to Ang II signaling (supplemental Tables I and II). Moreover, the analysis uncovered many novel phosphorylation sites as 32% of the regulated phosphorylation sites are not reported in public databases of known phosphosites (UniProt, PHOSIDA, and Phospho.ELM) (supplemental Tables I and II). We identified 3866 phosphorylation sites that are not previously reported in UniProt. Detailed information on all identified phosphosites is provided in supplemental Table III.

As depicted in Fig. 2*D*, the phosphoproteins regulated by Ang II affect a variety of different cellular functions. We manually assigned the phosphoproteins into functional groups based on their associated gene ontology terms, and the *inner circle* of Fig. 2*D* shows the overall distribution of phosphosites, whereas the *outer ring* of the *circle* illustrates the fraction of phosphosites regulated by Ang II only (*gray*) and phosphosites regulated by SII Ang II (*black*). These data demonstrate a previously unappreciated versatility of $G\alpha_q$-independent signaling and participation in Ang II-regulated cellular processes. According to this observation, the description "G protein-coupled receptors" can be misleading, whereas "7TM receptors" may be more accurate.

$G\alpha_q$-dependent and -independent Signaling Activates Different Kinases—The protein kinases are the backbone in cellular signaling pathways by transmitting signals from the plasma membrane to intracellular proteins through site-specific phosphorylation cascades. We identified 100 reproducibly up-regulated phosphorylation sites positioned on 42 kinases (Table I and see Fig. 5). Of these kinases, 23 have not previously been described in Ang II signaling. SII Ang II stimulation increased phosphorylation levels of 19 kinases. Although including mostly well known Ang II-regulated kinases, 14 of these kinases were not known to be regulated independently of $G\alpha_q$ protein. To evaluate the reproducibility of phosphorylation levels of phosphosites found in both biological replicates, we performed a Pearson's analysis of correlation. Regulation of phosphorylation sites on kinases was highly reproducible, showing a correlation of $r^2 = 0.90$ between the two biological replicates performed (Fig. 3*A*).

Comparing linear sequence motifs surrounding the regulated phosphorylation sites revealed differences in protein kinases activated by Ang II only (G protein-dependent) and Ang II plus SII Ang II (G protein-independent). Both Ang II signaling through $G\alpha_q$-dependent and -independent pathways preferentially stimulated phosphorylation of a basophilic AGC/CAM kinase motif ((R/K)*XX*p(S/T) where p represents phosphorylation) (Fig. 3*B*, *upper panel*). Indeed, among the 19 kinases phosphorylated by SII Ang II, 10 of them belong to the AGC/CAM kinase family, and seven of the 23 Ang II kinases regulated by Ang II only are AGC/CAM kinases. Interestingly, the phosphorylation of a proline-directed Erk-like phosphorylation motif (P*X*p(S/T)P) was only significant among the peptides that were regulated by Ang II in a $G\alpha_q$-dependent manner (Fig. 3*B*, *middle panel*). This remarkable observation of divergence could reflect that Erk1/2 translocates very fast to the nucleus upon $G\alpha_q$-dependent activation to reach its nuclear substrates, whereas it is tied up in the cytosol by β-arrestin and activates AGC- and CAM-like kinases after $G\alpha_q$-independent activation. As we discuss in detail below, the PKD consensus motif ((L/V/I/M)*XR XX*p(S/T)) was by far the most predominant motif within the group of SII Ang II-regulated peptides and was also over-represented among the Ang II-regulated peptides, indicating substantial PKD activity. The AGC/CAM kinases CAMK2δ and PKD have previously been found in association with β-arrestin 2, supporting their role in $G\alpha_q$-independent Ang II signaling (40).

To validate that the Mascot Score for peptide identification did not influence the data interpretation, we investigated whether the motif analysis was related to certainty of peptide identification by applying a filter on the sites identified based on a Mascot score cutoff of 48.9, equal to the upper 25% quantile and reapplying the motif analysis. The most significant feature was still the AGC/CAM motif for both sites regulated uniquely by Ang II (33% or 70 of 212 sites) and for sites regulated by both SII and Ang II (42% or 42 of 100 sites). This compares with a non-regulated background where this motif was found in only 14.8% or 331 of 2229 sites. The subset of these sites containing the PKD substrate motif was still significant for both uniquely Ang II-regulated sites (11% or 24 of 212 sites) and sites regulated by both SII and Ang II (14% or 14 of 100 sites) compared with a background of non-regulated sites (2.7% or 60 of 2229 sites). However, the Erk motif was no longer significant; although by closer analysis, the same trend was seen (8.9% of sites uniquely regulated by Ang II compared with a background of 4.8%). This analysis convincingly demonstrates that the Mascot score of a given peptide does not influence the likelihood of it being determined as regulated. The results also show that the motif analysis is limited in sensitivity given fewer sites but a differing Mascot score does not affect the motif extracted.

Transactivation of Membrane Receptors by Ang II—Ang II is known to influence activation and signal transduction of several other plasma membrane receptors, for example the EGF receptor (41, 42). Our data show reproducible transphosphorylation of 10 membrane receptors, six of which depend on $G\alpha_q$ protein activation, whereas four were phosphorylated independently of the $G\alpha_q$ signaling (Table II). Ang II stimulation

TABLE I
Regulated protein kinases

Amino acids are numbered according to UniProt numbering. Proteins that have not previously been linked to Ang II signaling are depicted in bold. Phosphorylation sites not reported in UniProt, PHOSIDA, and Phospho.Elm are depicted in bold. Phosphorylation sites also regulated by Ang II in the SII Ang list are shown in italics. MAPK, mitogen-activated protein kinase.

Gene	Protein name	Phosphosite	Maximum Ang II fold change	Maximum SII Ang II fold change
Angiotensin II-regulated				
PKN1	Protein kinase N1	**Ser^{372}, Ser^{380}**	>20	0.9
ADRBK1	G protein-coupled receptor kinase 2	Ser^{685}	>20	1.4
RPS6KB2	p70 S6 kinase β	Ser^{416}, Ser^{417}, Ser^{423}	18.9	1.6
EPHA2	Ephrin type A receptor 2	Ser^{897}, Ser^{901}	17.7	3.17
ITPKB	Inositol trisphosphate 3-kinase B	Ser^{43}, Ser^{49}	16.1	0.9
INSR	Insulin receptor	Ser^{1354}	11.1	1.6
NEK7	Protein kinase Nek7	Thr^{190}, Ser^{195}	9.4	1.4
RIPK2	Receptor-interacting kinase2	Ser^{531}	9.0	1.8
CDC42BPA	Ser/Thr Protein kinase MRCKα	Ser^{1673}, Ser^{1676}	7.9	3.2
ROCK2	Rho-associated protein kinase 2	Ser^{1137}	7.1	1.3
PRKAR2A	cAMP-dependent protein kinase 2α	Ser^{58}	6.5	0.8
TTBK2	Tau-tubulin kinase	**Ser^{850}, Ser^{853}**	6.2	1.5
PRKAA1	5′-AMP-activated protein kinase α1	Ser^{497}	5.5	1.3
TRIO	Triple functional domain protein	Ser^{2396}, **Ser^{2400}**	5.5	1.6
BUB1	Mitotic checkpoint kinase BUB1	Ser^{596}	4.7	1.3
WNK1	Ser/Thr Protein kinase WNK1	**Ser^{2372}**	4.5	1.1
SRPK2	Ser/Thr Protein kinase SRPK2	Ser^{494}, Ser^{497}	3.9	1.5
LATS1	Ser/Thr Protein kinase LATS1	Ser^{462}, Ser^{464}	3.5	1.5
BMP2K	BMP-2-inducible protein kinase	Ser^{1029}, Ser^{1031}, Ser^{1032}	3.4	1.4
PCTK1	Ser/Thr Protein kinase PCTAIRE-1	Ser^{116}, Ser^{153}	3.0	1.3
TESK2	Dual specificity testis-specific protein kinase 2	**Ser^{369}**	2.1	1.0
BRAF	Ser/Thr Protein kinase B-Raf	Ser^{151}	2.0	1.1
MAP2K2	Dual specificity mitogen-activated protein kinase kinase 2	Thr^{394}, Thr^{396}	1.7	1.2
SII angiotensin II-regulated				
STK10[a]	Ser/Thr-protein kinase 10	Ser^{13}, Thr^{14}, Ser^{450}, Ser^{454}, Ser^{455}	>20	13.8
PRKD2[a]	Protein kinase D2	Ser^{197}, Ser^{198}, Thr^{199}, Ser^{203}, *Ser^{396}*	>20	4.2
RSK1[a]	Ribosomal protein S6 kinase α1	*Thr^{359}, Ser^{363}, Ser^{369}*, Ser^{732}, **Ser^{733}**	>20	3.4
MSK1[a]	Glycogen synthase kinase 3 homolog MSK-1	Ser^{376}, Ser^{381}	>20	3.8
ERK1	Extracellular signal-regulated kinase 1	Thr^{198}, Thr^{202}, Tyr^{204}	>20	4.3
ERK2	Extracellular signal-regulated kinase 2	Thr^{185}, Tyr^{187}	>20	3.6
ARAF[a]	Ser/Thr protein kinase A-Raf	Thr^{181}, Ser^{186}	16.8	3.1
CAMK2D[a]	Calmodulin-dependent protein kinase 2δ	Ser^{330}, Ser^{333}, Ser^{334}, Ser^{337}	15.8	7.4
RSK2	Ribosomal protein S6 kinase α3	Thr^{365}, Ser^{369}, Ser^{375}	14.1	6.7
RPS6KB1[a]	p70 S6 kinase α	Ser^{441}, Thr^{444}, Ser^{205}	12.7	4.0
PRKD1[a]	Protein kinase D1	Ser^{205}, Ser^{208}, Ser^{210}, ***Ser^{237}***, Thr^{395}, Ser^{397}, Ser^{401}	12.3	2.5
MARK2[a]	Microtubule affinity-regulating kinase 2	Ser^{6}, *Ser^{9}, Thr^{596}*	11.5	2.2
MEKK3	MAPK/Erk kinase kinase 3	Ser^{197}, Ser^{206}, Ser^{207}, Ser^{368}, Ser^{371}	9.1	5.5
SLK[a]	STE20-like Ser/Thr-protein kinase	Ser^{340}, *Ser^{344}, Ser^{347}, Ser^{348}*	6.7	3.1
FYN	Proto-oncogene protein kinase Fyn	Ser^{21}, *Ser^{26}*	5.9	1.9
RET[a]	Proto-oncogene protein kinase Ret	Ser^{83}	5.8	2.7
FGFR3[a]	Fibroblast growth factor receptor 3	**Ser^{532}, Ser^{533}, Thr^{538}**	5.0	2.3
PRKD3[a]	Protein kinase D3	Ser^{41}, Ser^{44}	3.3	2.2
BRSK2[a]	BR serine/threonine-protein kinase 2	**Ser^{416}**	3.3	1.9

[a] Proteins not previously described to be regulated independently of G protein activation.

induced phosphorylation of both the insulin and IGF2 receptors. This is interesting, because several pieces of clinical and biological evidence indicate cross-talk between AT_1R and insulin receptor signaling (43, 44), but to our knowledge a direct link at the receptor level has not been reported. Furthermore, phosphorylation independent of $G\alpha_q$ protein activation was also seen on three previously undiscovered FGF receptor phosphorylation sites. Ang II also resulted in phosphorylation of other 7TMRs including the β_2-adrenergic receptor, which is an AT_1R interaction partner on a functional level (45).

Protein Kinase D Is a Key Protein Kinase in $G\alpha_q$ Protein-independent Ang II Signaling—The group of kinases that were phosphorylated after SII Ang II stimulation includes all three isoforms of PKD (Table I). Furthermore, we found 52 SII Ang II-up-regulated phosphorylation sites, which all conform to the PKD consensus phosphorylation motif (V/L/I)*X*R*XX*(S/T)

A

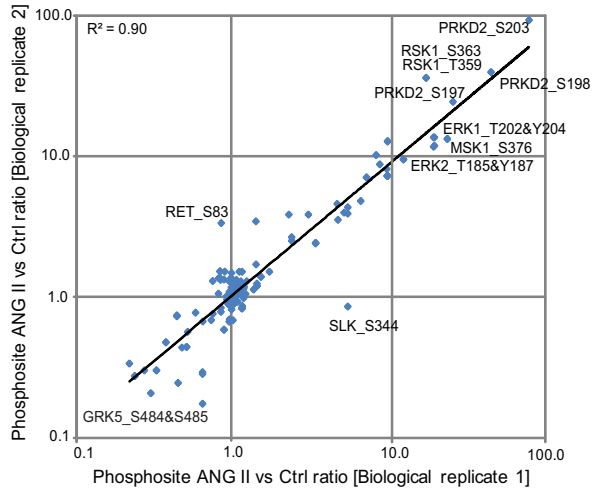

B

Ang II and SII Ang II specific

AGC and CAM substrate motif [R/K-X-X-pS/T]

ANG, not SII regulated: 33.9% (256 sites)*
ANG and SII regulated: 39.0% (144 sites)*
Not regulated: 21.0% (1605 sites)

Ang II specific

Erk1/2 substrate motif [P-X-pS/T-P]

ANG, not SII regulated: 11.0% (83 sites)*
ANG and SII regulated: 5.1% (19 sites)
Not regulated: 6.2% (476 sites)

Ang II and SII Ang II specific

PKD substrate motif [L/V/I/M-X-R/K-X-X-pS/T]

ANG, not SII regulated: 10.1% (76 sites)*
ANG and SII regulated: 14.1% (52 sites)*
Not regulated: 3.4% (262 sites)

(46), pointing to a substantial activation of PKD and phosphorylation of its substrates (Fig. 3*B*). The 52 putative PKD phosphorylation sites and protein substrates are depicted in supplemental Table VI.

Because of the potentially large impact of PKD activation, we further explored how PKDs are regulated by $G\alpha_q$-independent signaling. First we validated whether the observed phosphorylation of PKD isoforms leads to their activation by performing Western blot analysis on lysates from Ang II- and SII Ang II-treated cells. We used a phosphospecific antibody against the autophosphorylation site, serine 910, which is known to correlate with the kinase activity of PKD1. As depicted in Fig. 4*A*, both Ang II and SII Ang II stimulation induced a robust phosphorylation of serine 910. Furthermore, the autophosphorylation of PKD1 and the activity of PKD1 measured in a PKD1 kinase activity assay (Fig. 4*C*) showed that both Ang II and SII Ang II rapidly and robustly activated the PKD1.

PKD activation has been described to be mediated by novel PKC family members (47, 48). PKCs are central Ang II-regulated kinases. It was previously shown that Ang II activates PKD through PKCδ (47), but until now, this activation has been considered $G\alpha_q$-dependent. The SII Ang II-mediated PKD activation is also dependent on PKCδ as it is was sensitive to the PKC inhibitor Gö6983 and the PKCδ-specific inhibitor rottlerin (Fig. 4*B*). PKCδ was activated by both Ang II and SII Ang II, which were evaluated by immunoblotting against phospho-Thr^{507} (data not shown), which is the kinase domain activation site. In contrast to SII Ang II activation of PKD, activation by Ang II appears to be dependent on other PKC isotypes as it was more effectively blocked with the broader PKC inhibitor Gö6983 than with the PKCδ-specific rottlerin (Fig. 4*B*).

A well known pathway leading to PKCδ activation is activation of Rho and ROCK (49, 50). Considering the large

FIG. 3. **Kinase regulation.** *A*, the regulation level of phosphorylation on protein kinases was very reproducible between the two biological replicates. A -fold change plot of the Ang II *versus* control ratio from the first biological replicate against the second reveals an impressive reproducibility resulting in a correlation of $r^2 = 0.9$. *B*, $G\alpha_q$-dependently and -independently activated kinases phosphorylate distinct motifs. *Top panel*, among both the Ang II- and the SII Ang II-regulated peptides more than a third of the phosphorylation sites observed to be regulated were on the AGC/CAM kinase motif R*XX*p(S/T). *Middle panel*, the Erk1/2 kinase motif P*X*p(S/T)P is specific for the peptides that are only regulated by Ang II; *i.e.* of the G protein-dependently phosphorylated peptides, 83 of the peptides in the Ang II only group were phosphorylated on an Erk1/2 motif. *Bottom panel*, a further analysis of the SII Ang II-regulated peptides matching the AGC/CAM kinase motif showed that the dominant phosphorylation site within this group matched the PKD consensus motif ((V/L/I)*X*R*XX*(S/T)). * indicates statistically significant over-representation compared with non-regulated phosphopeptides. Statistically significant over-representation was calculated using the R implementation of Fisher's exact test. *Ctrl*, control; *ANG*, Ang II SII, SII Ang.

TABLE II
Phosphorylated membrane receptors

Amino acids are numbered according to UniProt numbering. Proteins that have not previously been linked to Ang II signaling are depicted in bold. Phosphorylation sites not reported in UniProt, PHOSIDA, and Phospho.Elm are depicted in bold.

Gene	Protein name	Phosphosite	Maximum Ang II fold change	Maximum SII Ang II fold change
Angiotensin II-regulated				
EPHA2	Ephrin type A receptor 2	Ser^{897}, Ser^{901}	17.7	3.1
ADRB2	β_2-Adrenergic receptor	Ser^{246}	13.5	1.6
CXADR	Coxsackievirus and adenovirus receptor	Ser^{293}, **Ser^{301}, Ser^{304}**	11.1	1.0
INSR	Insulin receptor	Ser^{1354}	11.1	1.6
S1PR2	Sphingosine 1-phosphate receptor 2	**Ser^{330}, Ser^{332}, Ser^{333}**	5.1	1.1
IGF2R	Insulin-like growth factor 2 receptor	Ser^{2401}, Ser^{2409}	2.7	1.3
SII angiotensin II-regulated				
PAR2	Proteinase-activated receptor 2	**Ser^{383}, Ser^{384}, Ser^{385}, *Ser^{387}*, Ser^{388}, Ser^{390}**	16.9	9.1
LPHN2	Latrophilin-2	**Ser^{1112}, Ser^{1115}**	14.9	3.3
CXCR4	CXC chemokine receptor type 4	Ser^{324}, Ser^{325}	7.8	3.6
FGFR3	Fibroblast growth factor receptor 3	**Ser^{532}, Ser^{533}, Thr^{538}**	5.0	2.3

amount of phosphorylated GEFs and GTPase-activating proteins in our data, we believe that the observed PKCδ and PKD activation could be a result of ROCK activity. The mechanism of small GTPase activation by the AT_1R has been poorly elucidated. The anchoring protein AKAP13, which is also highly phosphorylated by SII Ang II, has been shown to function as a GEF for Rho and simultaneously to interact with both PKCδ and PKD, perhaps as a scaffold to bring the two kinases in close proximity (51). To test whether the observed PKD activation was ROCK-dependent, we measured PKD activation by the ability of PKD to phosphorylate syntide 2 in the presence of the ROCK-specific inhibitor Y27632. As depicted in Fig. 4*C*, the ROCK inhibitor inhibited 94% of the SII Ang II-mediated PKD activation and only 45% of the Ang II-mediated PKD activation. These data suggest a model where Rho/ROCK/PKCδ/PKD is activated independently of $G\alpha_q$ activation (Fig. 4*D*).

DISCUSSION

In this study, we identified more than 500 phosphoproteins regulated by Ang II of which the majority has not previously been implicated in Ang II signaling (supplemental Tables I and II and Fig. 2). Importantly, our data reveal a previously unexpected amount and versatility of $G\alpha_q$-independent signaling because SII Ang II regulated 36% of the AT_1R-regulated phosphosites and affected the same cellular functions as the $G\alpha_q$-dependent part of the signaling (Fig. 2). Furthermore, $G\alpha_q$-dependent and -independent AT_1R signaling pathways are very distinct as reflected by activation of different kinds of kinases. This was observed as both phosphorylation of the actual kinases and "fingerprints" that activated kinases leave on other phosphorylated substrate proteins due to their peptide motif specificity (Table I and Fig. 3*B*).

Quite unexpectedly, we observed that Ang II signaling almost exclusively occurs through serine (88.3%) and threonine (11.1%) phosphorylation (Fig. 2*B* and supplemental Tables I and II). We observed very little tyrosine phosphorylation (0.6%) and only identified regulation of five tyrosine kinases (EPHA2, FYN, insulin receptor, RET, and FGFR3) (Table I). However, there is no doubt that other tyrosine kinases such as the Jak and Src kinases as well as EGF receptor tyrosine kinase are important mediators of AT_1R signaling in certain cellular conditions (6, 11, 13, 52–54). In a similar large scale phosphoproteomics analysis of the EGF receptor, we found that 6% of the regulated phosphosites were Tyr(P) (26). This provides assurance that our method is able to detect tyrosine phosphorylation sites, and therefore our data indicate that EGF receptor transactivation and tyrosine kinase signaling may play a minor role in AT_1R signaling in HEK293 cells that might to some extent be due to low expression of EGF receptors.

This unbiased mass spectrometric analysis uncovered unexpected regulation of specific phosphorylation patterns and proteins in the two AT_1R signaling pathways. We showed that PKD was activated by SII Ang II through PKCδ- and ROCK-dependent signal transduction, whereas Ang II activation of PKD via $G\alpha_q$ protein may also depend on other PKCs (Fig. 4*D*). These data challenge the understanding of PKCs as strictly $G\alpha_q$-dependent regulated kinases in the Ang II system and place PKD as a very central hub in $G\alpha_q$-independent mediated signal transduction from the AT_1R. PKD has not attracted much attention in cardiovascular signaling compared with its relatives in the PKC family. However, emerging data point to a central role for PKDs in AT_1R-regulated signal transduction, resulting in the induction of cardiac hypertrophy as well as in protection against apoptosis, migration, remodeling, and proliferation (55, 56). The regulation of these very different cellular outcomes is presumably related to distinct cellular localization of the PKD isoforms and organization into different signalosomes (56). Interestingly, this study showed that PKD can also be regulated by

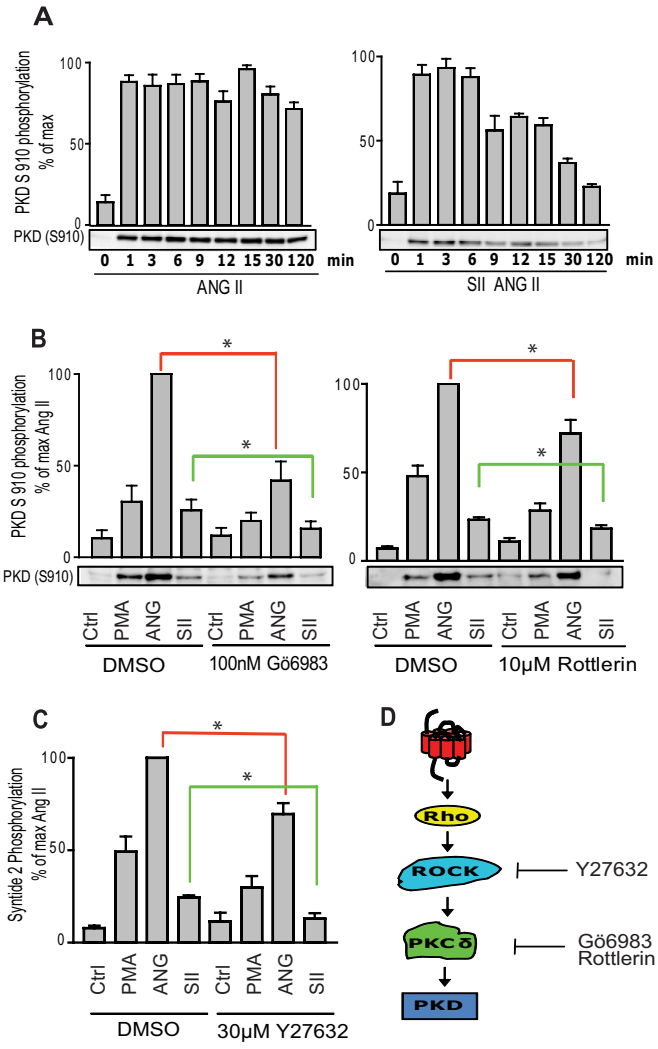

FIG. 4. **PKD activation depends on ROCK/PKCδ activity.** *A*, Western blots showing increased phosphorylation of the autophosphorylation site Ser^{910} on PKD1 upon treatment with 10 nM Ang II and 1.87 μM SII Ang II for 0–120 min. Data are presented as the mean and error bars reflect ± S.E. of four experiments. *B*, Western blots showing inhibition of PKD1 Ser^{910} phosphorylation upon Ang II and SII Ang II treatment in the presence of the PKC inhibitor Gö6983 and the PKCδ-specific inhibitor rottlerin. The statistical difference between Ang II and SII Ang II with and without inhibitors was tested with a one-tailed paired Student's *t* test. *, $p < 0.05$. Data are presented as the mean and error bars reflect ± S.E. of three experiments. *C*, kinase assay showing phosphorylation of the PKD substrate peptide syntide 2 in the presence and absence of 30 μM ROCK inhibitor Y27632. AT_1R-HEK cells were starved overnight and pretreated with Y27632 for 30 min before stimulation with 10 nM Ang II and 1.87 μM SII Ang II for 3 min. Lysates were immunoprecipitated with anti-PKD antibody, and syntide 2 peptide was subjected to phosphorylation for 10 min in the presence of [^{32}P]ATP. Syntide 2 was spotted to Whatmann paper and washed thoroughly before autoradiography. The statistical difference between Ang II and SII Ang II with and without inhibitors was tested with a one-tailed paired Student's *t* test. *, $p < 0.05$. Data are presented as the mean and error bars reflect ± S.E. of three experiments. *D*, schematic indicating the G protein-independent pathway to PKD activation going through Rho/ROCK/PKCδ. *ANG*, Ang II; *PMA*, phorbol 12-myristate 13-acetate; *max*, maximum.

$G\alpha_q$-independent mechanisms via the Rho/ROCK pathway. A substantial fraction of the Ang II-regulated proteins displayed here is involved in small GTPase activation, plasma membrane remodeling, and cytoskeletal rearrangements. In general, we found many GEFs and GTPase-activating proteins in both groups, indicating a substantial activity of small GTPase signaling. We believe that a focus on small GTPases may reveal a novel branch of the G protein-independent signaling network.

In recent years, research on Ang II has been focused on the cellular phenotypes resulting from G protein-dependent *versus* β-arrestin-dependent signal transduction. Cellular outcomes such as gene expression changes, proliferation, migration, apoptosis, and hypertrophy have been linked to Ang II signaling (22, 24, 40, 57). A study of Ang II-mediated transcriptional changes concluded that transcriptional regulation is dependent on $G\alpha_q$ activation and inhibited by β-arrestins (58). In support of this observation, we found that Ang II up-regulated phosphorylation of several transcription factors, for example c-JUN, HOXA3, and EP400 in a strictly $G\alpha_q$-dependent manner (supplemental Table I). On the other hand, we also measured an extensive SII Ang II-stimulated phosphorylation site regulation of nuclear proteins, strongly indicating that the $G\alpha_q$-independent signal is somehow propagated to the nucleus (supplemental Table II). As the β-arrestin-dependent signal to the nucleus does presumably not induce transcriptional activation, it could instead mediate transcriptional repression. Indeed, we observed SII Ang II-regulated phosphorylation of transcriptional regulators such as LARP, MIER, and TRIM33 that are known to mediate transcriptional repression. SII Ang II also regulated the programmed cell death protein 4 (PDCD4) at several sites including Ser^{67}. It has been shown that upon Ser^{67} phosphorylation PDCD4 translocates to the nucleus and represses c-JUN- and β-catenin-mediated transcription (59). PDCD4 has also been proposed to form a complex with β-arrestins 1 and 2 (40). The lack of transcriptional activity upon β-arrestin signaling may also be due to nuclear exclusion of proteins central for progression of the transcriptional process. One example is CAMK2δ, which is involved in both growth responses and transcriptional regulation. CAMK2δ is phosphorylated on multiple sites by SII Ang II stimulation in a cluster (Ser^{330}–Thr^{337}) adjacent to the nuclear localization signal, possibly inhibiting nuclear translocation of CAMK2δ (60).

SII Ang II stimulates protein synthesis in both HEK293 and vascular smooth muscle cells by activation of the translation initiator EIF4A (61). In agreement with this finding, we observed phosphorylation on EIF4B and EIF5B on multiple sites by both Ang II and SII Ang II. We also observed Ang II-stimulated phosphorylation on 12 proteins involved in the ubiquitination-mediated protein degradation process (supplemental Table I). Only three of these proteins (calpastatin and the ubiquitin ligases TRIM33 and PRAJA1) were affected by SII Ang II stimulation (supplemental Table II).

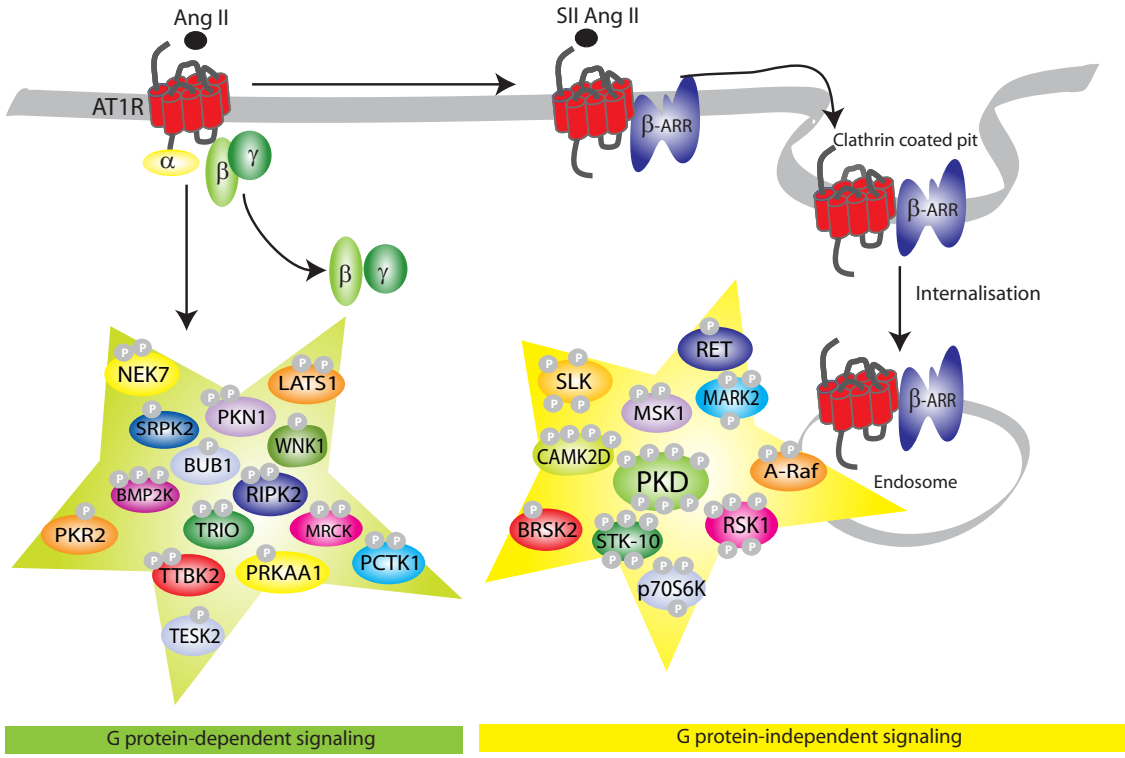

FIG. 5. **Novel kinases in AT1R signaling.** The illustration depicts the novel AT_1R-regulated kinases identified in this study. Note that the kinases illustrated as G protein-independent may be activated by both pathways, whereas the kinases regulated strictly by Ang II are considered as G protein-dependent. *β-ARR*, β-arrestin.

In the Ang II signaling system, $G\alpha_q$-dependent mechanisms have been reported to increase apoptosis, whereas β-arrestin-mediated signaling may protect against apoptosis (57). We found ligand-regulated phosphorylation of both pro- and antiapoptotic proteins by Ang II (*e.g.* proapoptotic protein reticulon 4 (NOGO) and the antiapoptotic BCL-2 family member BIS) as well as SII Ang II (*e.g.* the well known antiapoptotic kinases RSK2 and p70S6K and the antiapoptotic protein PEA-15 as well as the proapoptotic DIDO-1).

We found a variety of proteins involved in cell cycle regulation to be involved in both $G\alpha_q$-dependent and -independent signaling. DNA polymerase 1 (POLA1) was phosphorylated in a strictly $G\alpha_q$-dependent manner on Ser^{192}, a previous unidentified phosphorylation site. The nuclear interaction partner of anaplastic lymphoma kinase (NIPA) was phosphorylated by SII Ang II on a cluster of 7 residues including Ser^{354} and Ser^{359}, which most likely results in degradation of the nuclear interaction partner of anaplastic lymphoma kinase and accumulation of cyclin B in late G_2, which in theory leads to cell cycle progression (27). However, SII Ang II did not result in proliferation in the AT_1R-HEK cells (data not shown) as was observed in cardiac myocytes and NIH3T3 cells (22, 39).

Upon AT_1R activation, the formation of clathrin-coated pits and receptor endocytosis are initiated, which require a considerable rearrangement of the cytoskeleton. Here, we observed that dynamin, filamin A, and vimentin, which are central filamentous proteins involved in endocytosis, F-actin polymerization, and migration, were regulated strictly by Ang II. Contradictory, cellular migration toward an attracting chemical factor (chemotaxis) has been directly related to β-arrestin 2-dependent AT_1R signaling (24). Numerous proteins involved in the endocytosis and cytoskeletal reorganization were regulated by SII Ang II including GIT1, REPS1, and PACS1.

CONCLUSIONS

This is the first study dissecting the differences between a full agonist and a biased agonist of a 7TMR by mass spectrometry. Using a high resolution and quantitative mass spectrometric approach, we identified more than 500 phosphoproteins regulated by Ang II of which the majority has not previously been implicated in Ang II signaling. Our data reveal a previously unexpected amount and versatility of $G\alpha_q$-independent signaling from this 7TMR because SII Ang II affected 36% of the identified AT_1R signaling network and influenced all Ang II-regulated cellular events. In addition, we also established that the two signaling pathways are in fact very distinct in their nature, which is reflected by activation of different protein kinases. The shotgun mass spectrometric approach did not uncover all proteins in the network but provided multiple pieces of the puzzle. For many proteins such as PKD, this unbiased analysis uncovered unexpected regulation patterns

and exposed proteins not previously considered to be a part of the Ang II signaling network (Fig. 5). We believe that this mapping of the Ang II signalosome will serve as a basis for future studies on the regulation of Ang II signaling molecules as well as provide a broader and more in-depth overview of the effect on cellular outcomes mediated by different AT_1R signaling pathways, which could be important for the pharmacological use of biased agonists in cardiovascular diseases. Looking at AT_1R signaling as a model system for 7TMR signaling in general, the amount and diversity of $G\alpha_q$-independent signaling may be larger than previously acknowledged in other systems as well. Moreover, our study holds promise for quantitative mass spectrometry as a universal tool in the evaluation and analysis of biased agonists to other receptors in the future.

Acknowledgments—We thank Birte Kofoed for excellent technical assistance and Robert J. Lefkowitz for kindly providing us with the stable transfected AT_1R-HEK cells. The Centre for Protein Research is funded by a generous donation by the Novo Nordisk Foundation.

* This work was supported by The Danish National Research Foundation, The Købmand i Odense Johan og Hanne Weimann f. Seedorffs legat, The Danish Heart Foundation, the Novo Nordisk Foundation, The Augustinus Foundation, and the Aase og Ejnar Danielsens Foundation.

The raw data associated with this manuscript may be downloaded from ProteomeCommons.org Tranche, https://proteomecommons.org/tranche/, using the following hash codes: all spectra: AkG/I6DDb4N6PFouQySWFB7f0vNPdfzVN0sQ/wDFPxdBDYschQp+0fvbHAd6C9MWlHa+e1hOm9ZK3X1itkM7m/B1MywAAAAAAABVtw==; pass phrase, ANG2gitte; and annotated spectra: 8dTCR89xDMxbL7j4fbhHDxs/6463EzqsuTfURzr/NBCG3b/3d0Sb8UWDFm7khvibmcuhEV1sZYrufaPR7uxmDwY68mYAAAAAAAACzw==; pass phrase, ANG2gitte.

S This article contains the following supplemental data: Table I, phosphopeptides regulated by Ang II alone; Table II, phosphopeptides regulated by ANG II plus SII Ang II; Table III, phosphopeptides regulated by SII Ang II alone; Table IV, all regulated phosphopeptides; Table V, all peptides; Table VI, protein kinase D motif peptides; Table VII, all proteins; Table VIII, all modified peptides; Data IX, annotated MS/MS spectra of regulated phosphosites; Fig. X, coverage of fragment ions; and Fig. XI, comparison of Mascot scores for regulated *versus* non-regulated peptides.

‖ Both authors contributed equally to this work.

¶¶ To whom correspondence may be addressed: Novo Nordisk Foundation Center for Protein Research, Faculty of Health Sciences, University of Copenhagen, Blegdamsvej 3b, DK-2200 Copenhagen, Denmark. Tel.: 45-3532-5022; Fax: 45-3532-5001; E-mail: jesper.olsen@cpr.ku.dk.

‖‖ To whom correspondence may be addressed: Laboratory for Molecular Cardiology, The Danish National Research Foundation Centre for Cardiac Arrhythmia, Department of Biomedical Sciences, University of Copenhagen, Blegdamsvej 3b, DK-2200 Copenhagen, Denmark. Tel.: 45-3532-7645; Fax: 45-3532-7610; E-mail: jlhansen@sund.ku.dk.

REFERENCES

1. Urban, J. D., Clarke, W. P., von Zastrow, M., Nichols, D. E., Kobilka, B., Weinstein, H., Javitch, J. A., Roth, B. L., Christopoulos, A., Sexton, P. M., Miller, K. J., Spedding, M., and Mailman, R. B. (2007) Functional selectivity and classical concepts of quantitative pharmacology. *J. Pharmacol. Exp. Ther.* **320,** 1–13
2. Violin, J. D., and Lefkowitz, R. J. (2007) Beta-arrestin-biased ligands at seven-transmembrane receptors. *Trends Pharmacol. Sci.* **28,** 416–422
3. Aplin, M., Christensen, G. L., and Hansen, J. L. (2008) Pharmacologic perspectives of functional selectivity by the angiotensin II type 1 receptor. *Trends Cardiovasc. Med.* **18,** 305–312
4. Schmid, C. L., Raehal, K. M., and Bohn, L. M. (2008) Agonist-directed signaling of the serotonin 2A receptor depends on beta-arrestin-2 interactions in vivo. *Proc. Natl. Acad. Sci. U.S.A.* **105,** 1079–1084
5. Abbas, A., and Roth, B. L. (2008) Arresting serotonin. *Proc. Natl. Acad. Sci. U.S.A.* **105,** 831–832
6. Ali, M. S., Sayeski, P. P., Dirksen, L. B., Hayzer, D. J., Marrero, M. B., and Bernstein, K. E. (1997) Dependence on the motif YIPP for the physical association of Jak2 kinase with the intracellular carboxyl tail of the angiotensin II AT1 receptor. *J. Biol. Chem.* **272,** 23382–23388
7. Schlaepfer, D. D., Jones, K. C., and Hunter, T. (1998) Multiple Grb2-mediated integrin-stimulated signaling pathways to ERK2/mitogen-activated protein kinase: summation of both c-Src- and focal adhesion kinase-initiated tyrosine phosphorylation events. *Mol. Cell. Biol.* **18,** 2571–2585
8. Shukla, A. K., Violin, J. D., Whalen, E. J., Gesty-Palmer, D., Shenoy, S. K., and Lefkowitz, R. J. (2008) Distinct conformational changes in beta-arrestin report biased agonism at seven-transmembrane receptors. *Proc. Natl. Acad. Sci. U.S.A.* **105,** 9988–9993
9. Kenakin, T. (2005) New concepts in drug discovery: collateral efficacy and permissive antagonism. *Nat. Rev. Drug Discov.* **4,** 919–927
10. Wisler, J. W., DeWire, S. M., Whalen, E. J., Violin, J. D., Drake, M. T., Ahn, S., Shenoy, S. K., and Lefkowitz, R. J. (2007) A unique mechanism of beta-blocker action: carvedilol stimulates beta-arrestin signaling. *Proc. Natl. Acad. Sci. U.S.A.* **104,** 16657–16662
11. Mehta, P. K., and Griendling, K. K. (2007) Angiotensin II cell signaling: physiological and pathological effects in the cardiovascular system. *Am. J. Physiol. Cell Physiol.* **292,** C82–C97
12. Aplin, M., Bonde, M. M., and Hansen, J. L. (2009) Molecular determinants of angiotensin II type 1 receptor functional selectivity. *J. Mol. Cell. Cardiol.* **46,** 15–24
13. Hunyady, L., and Catt, K. J. (2006) Pleiotropic AT1 receptor signaling pathways mediating physiological and pathogenic actions of angiotensin II. *Mol. Endocrinol.* **20,** 953–970
14. Zhai, P., Yamamoto, M., Galeotti, J., Liu, J., Masurekar, M., Thaisz, J., Irie, K., Holle, E., Yu, X., Kupershmidt, S., Roden, D. M., Wagner, T., Yatani, A., Vatner, D. E., Vatner, S. F., and Sadoshima, J. (2005) Cardiac-specific overexpression of AT1 receptor mutant lacking G alpha q/G alpha i coupling causes hypertrophy and bradycardia in transgenic mice. *J. Clin. Investig.* **115,** 3045–3056
15. Rajagopal, K., Whalen, E. J., Violin, J. D., Stiber, J. A., Rosenberg, P. B., Premont, R. T., Coffman, T. M., Rockman, H. A., and Lefkowitz, R. J. (2006) Beta-arrestin2-mediated inotropic effects of the angiotensin II type 1A receptor in isolated cardiac myocytes. *Proc. Natl. Acad. Sci. U.S.A.* **103,** 16284–16289
16. Holloway, A. C., Qian, H., Pipolo, L., Ziogas, J., Miura, S., Karnik, S., Southwell, B. R., Lew, M. J., and Thomas, W. G. (2002) Side-chain substitutions within angiotensin II reveal different requirements for signaling, internalization, and phosphorylation of type 1A angiotensin receptors. *Mol. Pharmacol.* **61,** 768–777
17. Lu, H. K., Fern, R. J., Luthin, D., Linden, J., Liu, L. P., Cohen, C. J., and Barrett, P. Q. (1996) Angiotensin II stimulates T-type Ca2+ channel currents via activation of a G protein, Gi. *Am. J. Physiol. Cell Physiol.* **271,** C1340–C1349
18. Rattan, S., Puri, R. N., and Fan, Y. P. (2003) Involvement of rho and rho-associated kinase in sphincteric smooth muscle contraction by angiotensin II. *Exp. Biol. Med.* **228,** 972–981
19. Gohla, A., Schultz, G., and Offermanns, S. (2000) Role for G(12)/G(13) in agonist-induced vascular smooth muscle cell contraction. *Circ. Res.* **87,** 221–227
20. Ahn, S., Shenoy, S. K., Wei, H., and Lefkowitz, R. J. (2004) Differential kinetic and spatial patterns of beta-arrestin and G protein-mediated ERK activation by the angiotensin II receptor. *J. Biol. Chem.* **279,** 35518–35525
21. Aplin, M., Christensen, G. L., Schneider, M., Heydorn, A., Gammeltoft, S., Kjølbye, A. L., Sheikh, S. P., and Hansen, J. L. (2007) The angiotensin

type 1 receptor activates extracellular signal-regulated kinases 1 and 2 by G protein-dependent and -independent pathways in cardiac myocytes and Langendorff-perfused hearts. *Basic Clin. Pharmacol. Toxicol.* **100,** 289–295
22. Aplin, M., Christensen, G. L., Schneider, M., Heydorn, A., Gammeltoft, S., Kjølbye, A. L., Sheikh, S. P., and Hansen, J. L. (2007) Differential extracellular signal-regulated kinases 1 and 2 activation by the angiotensin type 1 receptor supports distinct phenotypes of cardiac myocytes. *Basic Clin. Pharmacol. Toxicol.* **100,** 296–301
23. Ahn, S., Kim, J., Hara, M. R., Ren, X. R., and Lefkowitz, R. J. (2009) {beta}-Arrestin-2 Mediates Anti-apoptotic Signaling through Regulation of BAD Phosphorylation. *J. Biol. Chem.* **284,** 8855–8865
24. Hunton, D. L., Barnes, W. G., Kim, J., Ren, X. R., Violin, J. D., Reiter, E., Milligan, G., Patel, D. D., and Lefkowitz, R. J. (2005) Beta-arrestin 2-dependent angiotensin II type 1A receptor-mediated pathway of chemotaxis. *Mol. Pharmacol.* **67,** 1229–1236
25. Macek, B., Mann, M., and Olsen, J. V. (2009) Global and site-specific quantitative phosphoproteomics: principles and applications. *Annu. Rev. Pharmacol. Toxicol.* **49,** 199–221
26. Olsen, J. V., Blagoev, B., Gnad, F., Macek, B., Kumar, C., Mortensen, P., and Mann, M. (2006) Global, in vivo, and site-specific phosphorylation dynamics in signaling networks. *Cell* **127,** 635–648
27. Bassermann, F., von Klitzing, C., Illert, A. L., Münch, S., Morris, S. W., Pagano, M., Peschel, C., and Duyster, J. (2007) Multisite phosphorylation of nuclear interaction partner of ALK (NIPA) at G2/M involves cyclin B1/Cdk1. *J. Biol. Chem.* **282,** 15965–15972
28. Jensen, A. A., Hansen, J. L., Sheikh, S. P., and Bräuner-Osborne, H. (2002) Probing intermolecular protein-protein interactions in the calcium-sensing receptor homodimer using bioluminescence resonance energy transfer (BRET). *Eur. J. Biochem.* **269,** 5076–5087
29. Schroeder, M. J., Shabanowitz, J., Schwartz, J. C., Hunt, D. F., and Coon, J. J. (2004) A neutral loss activation method for improved phosphopeptide sequence analysis by quadrupole ion trap mass spectrometry. *Anal. Chem.* **76,** 3590–3598
30. Olsen, J. V., de Godoy, L. M., Li, G., Macek, B., Mortensen, P., Pesch, R., Makarov, A., Lange, O., Horning, S., and Mann, M. (2005) Parts per million mass accuracy on an Orbitrap mass spectrometer via lock mass injection into a C-trap. *Mol. Cell. Proteomics* **4,** 2010–2021
31. Cox, J., Matic, I., Hilger, M., Nagaraj, N., Selbach, M., Olsen, J. V., and Mann, M. (2009) A practical guide to the MaxQuant computational platform for SILAC-based quantitative proteomics. *Nat. Protoc.* **4,** 698–705
32. Cox, J., and Mann, M. (2008) MaxQuant enables high peptide identification rates, individualized p.p.b.-range mass accuracies and proteome-wide protein quantification. *Nat. Biotechnol.* **26,** 1367–1372
33. Elias, J. E., and Gygi, S. P. (2007) Target-decoy search strategy for increased confidence in large-scale protein identifications by mass spectrometry. *Nat. Methods* **4,** 207–214
34. Köcher, T., Savitski, M. M., Nielsen, M. L., and Zubarev, R. A. (2006) PhosTShunter: a fast and reliable tool to detect phosphorylated peptides in liquid chromatography Fourier transform tandem mass spectrometry data sets. *J. Proteome Res.* **5,** 659–668
35. Soufi, B., Kelstrup, C. D., Stoehr, G., Fröhlich, F., Walther, T. C., and Olsen, J. V. (2009) Global analysis of the yeast osmotic stress response by quantitative proteomics. *Mol. Biosyst.* **5,** 1337–1346
36. Daub, H., Olsen, J. V., Bairlein, M., Gnad, F., Oppermann, F. S., Körner, R., Greff, Z., Kéri, G., Stemmann, O., and Mann, M. (2008) Kinase-selective enrichment enables quantitative phosphoproteomics of the kinome across the cell cycle. *Mol. Cell* **31,** 438–448
37. Pan, C., Gnad, F., Olsen, J. V., and Mann, M. (2008) Quantitative phosphoproteome analysis of a mouse liver cell line reveals specificity of phosphatase inhibitors. *Proteomics* **8,** 4534–4546
38. Pan, C., Olsen, J. V., Daub, H., and Mann, M. (2009) Global effects of kinase inhibitors on signaling networks revealed by quantitative phosphoproteomics. *Mol. Cell. Proteomics* **8,** 2796–2808
39. Hansen, J. L., Aplin, M., Hansen, J. T., Christensen, G. L., Bonde, M. M., Schneider, M., Haunsø, S., Schiffer, H. H., Burstein, E. S., Weiner, D. M., and Sheikh, S. P. (2008) The human angiotensin AT(1) receptor supports G protein-independent extracellular signal-regulated kinase 1/2 activation and cellular proliferation. *Eur. J. Pharmacol.* **590,** 255–263
40. Xiao, K., McClatchy, D. B., Shukla, A. K., Zhao, Y., Chen, M., Shenoy, S. K., Yates, J. R., 3rd, and Lefkowitz, R. J. (2007) Functional specialization of beta-arrestin interactions revealed by proteomic analysis. *Proc. Natl. Acad. Sci. U.S.A.* **104,** 12011–12016
41. Kagiyama, S., Eguchi, S., Frank, G. D., Inagami, T., Zhang, Y. C., and Phillips, M. I. (2002) Angiotensin II-induced cardiac hypertrophy and hypertension are attenuated by epidermal growth factor receptor antisense. *Circulation* **106,** 909–912
42. Thomas, W. G., Brandenburger, Y., Autelitano, D. J., Pham, T., Qian, H., and Hannan, R. D. (2002) Adenoviral-directed expression of the type 1A angiotensin receptor promotes cardiomyocyte hypertrophy via transactivation of the epidermal growth factor receptor. *Circ. Res.* **90,** 135–142
43. Horiuchi, M., Mogi, M., and Iwai, M. (2006) Signaling crosstalk angiotensin II receptor subtypes and insulin. *Endocr. J.* **53,** 1–5
44. Velloso, L. A., Folli, F., Perego, L., and Saad, M. J. (2006) The multi-faceted cross-talk between the insulin and angiotensin II signaling systems. *Diabetes Metab. Res. Rev.* **22,** 98–107
45. Lyngsø, C., Erikstrup, N., and Hansen, J. L. (2009) Functional interactions between 7TM receptors in the renin-angiotensin system—dimerization or crosstalk? *Mol. Cell. Endocrinol.* **302,** 203–212
46. Hutti, J. E., Jarrell, E. T., Chang, J. D., Abbott, D. W., Storz, P., Toker, A., Cantley, L. C., and Turk, B. E. (2004) A rapid method for determining protein kinase phosphorylation specificity. *Nat. Methods* **1,** 27–29
47. Tan, M., Xu, X., Ohba, M., and Cui, M. Z. (2004) Angiotensin II-induced protein kinase D activation is regulated by protein kinase Cdelta and mediated via the angiotensin II type 1 receptor in vascular smooth muscle cells. *Arterioscler. Thromb. Vasc. Biol.* **24,** 2271–2276
48. Rozengurt, E., Rey, O., and Waldron, R. T. (2005) Protein kinase D signaling. *J. Biol. Chem.* **280,** 13205–13208
49. Li, J., O'Connor, K. L., Greeley, G. H., Jr., Blackshear, P. J., Townsend, C. M., Jr., and Evers, B. M. (2005) Myristoylated alanine-rich C kinase substrate-mediated neurotensin release via protein kinase C-delta downstream of the Rho/ROK pathway. *J. Biol. Chem.* **280,** 8351–8357
50. Song, J., Li, J., Lulla, A., Evers, B. M., and Chung, D. H. (2006) Protein kinase D protects against oxidative stress-induced intestinal epithelial cell injury via Rho/ROK/PKC-delta pathway activation. *Am. J. Physiol. Cell Physiol.* **290,** C1469–C1476
51. Carnegie, G. K., Smith, F. D., McConnachie, G., Langeberg, L. K., and Scott, J. D. (2004) AKAP-Lbc nucleates a protein kinase D activation scaffold. *Mol. Cell* **15,** 889–899
52. Marrero, M. B., Schieffer, B., Paxton, W. G., Heerdt, L., Berk, B. C., Delafontaine, P., and Bernstein, K. E. (1995) Direct stimulation of Jak/STAT pathway by the angiotensin II AT1 receptor. *Nature* **375,** 247–250
53. Zhai, P., Galeotti, J., Liu, J., Holle, E., Yu, X., Wagner, T., and Sadoshima, J. (2006) An angiotensin II type 1 receptor mutant lacking epidermal growth factor receptor transactivation does not induce angiotensin II-mediated cardiac hypertrophy. *Circ. Res.* **99,** 528–536
54. Hunyady, L. (2009) Physiological and pathological actions of the renin-angiotensin system. *Mol. Cell. Endocrinol.* **302,** 109–110
55. Romero, D. G., Welsh, B. L., Gomez-Sanchez, E. P., Yanes, L. L., Rilli, S., and Gomez-Sanchez, C. E. (2006) Angiotensin II-mediated protein kinase D activation stimulates aldosterone and cortisol secretion in H295R human adrenocortical cells. *Endocrinology* **147,** 6046–6055
56. Avkiran, M., Rowland, A. J., Cuello, F., and Haworth, R. S. (2008) Protein kinase d in the cardiovascular system: emerging roles in health and disease. *Circ. Res.* **102,** 157–163
57. Revankar, C. M., Vines, C. M., Cimino, D. F., and Prossnitz, E. R. (2004) Arrestins block G protein-coupled receptor-mediated apoptosis. *J. Biol. Chem.* **279,** 24578–24584
58. Lee, M. H., El-Shewy, H. M., Luttrell, D. K., and Luttrell, L. M. (2008) Role of beta-arrestin-mediated desensitization and signaling in the control of angiotensin AT1a receptor-stimulated transcription. *J. Biol. Chem.* **283,** 2088–2097
59. Lankat-Buttgereit, B., and Göke, R. (2009) The tumour suppressor Pdcd4: recent advances in the elucidation of function and regulation. *Biol. Cell* **101,** 309–317
60. Heist, E. K., Srinivasan, M., and Schulman, H. (1998) Phosphorylation at the nuclear localization signal of Ca2+/calmodulin-dependent protein kinase II blocks its nuclear targeting. *J. Biol. Chem.* **273,** 19763–19771
61. DeWire, S. M., Kim, J., Whalen, E. J., Ahn, S., Chen, M., and Lefkowitz, R. J. (2008) Beta-arrestin-mediated signaling regulates protein synthesis. *J. Biol. Chem.* **283,** 10611–10620